Transformation of filter transmission data for f-number and chief ray angle

Jeffrey L. Rienstra

Sandia National Laboratories, P.O. Box 5800, MS 0972, Albuquerque, NM 87185-0972

ABSTRACT

This paper describes a method for transforming measured optical and infrared filter data for use with optical systems of arbitrary f-number and angle of incidence. Although it is generally desirable to have normal incidence at the filter (i.e., collimated light where an optical filter is used), other system design considerations may take precedence. In the case of a multispectral sensor under development at Sandia National Laboratories, system constraints require optical filter placement very near the focal plane. The light rays incident on the filters are therefore converging as determined by the system f-number while the chief ray of each ray bundle varies with focal plane position. To analyze the system's spectral response at different points on the focal plane, a method was devised to transform the filter vendor's measured data to account for the optical system design. The key to the transformation is the determination of weighting factors and shift factors for each angle of incidence making up a ray bundle. A computer worksheet was developed using a popular mathematical software package which performs this transformation for 75 key points on the focal plane.

Keywords: interference filters, multispectral imaging, remote sensing

1. INTRODUCTION

Sandia National Laboratories and a team of other national laboratories and contractors are building a multispectral sensor system which includes multilayer interference filters to define wavelength bands. These bandpass filters are located near the focal plane of the optical system. When interference filters are used it is usually desirable to use collimated light and keep the angle of incidence constant, since the spectral characteristics of these filters change with angle of incidence. Many tradeoffs were considered for this particular system, and an optical design was adopted in which the light incident on the filters is not collimated. A ray trace of the optical design shows converging ray bundles incident on the bandpass filters. The chief ray of each ray bundle varies with location on the focal plane. Since this is an imaging system, focal plane location maps to field angle and there is a slight spectral variation across the recorded image. The focal plane for this sensor system is cooled to less than 80 K, so any temperature effects on transmission must also be accounted for.

Analysis of the data from this multispectral sensor requires accurate knowledge of the spectral bandpass for each detector on the focal plane. It was impractical to measure the spectral characteristics at each of the hundreds of detector locations for each spectral band, so we identified a need to quickly calculate the filter transmission properties at different focal plane locations.

As part of the filter specification, the vendor was given the system f-number and a typical chief ray angle for each spectral band. This information guided the filter vendor so the appropriate spectral shift could be built into the filter design. The filter vendor measured the spectral characteristics of the delivered filters using a nearly collimated, high f-number spectroradiometer. The vendor also measured witness samples of the filters at approximately 80 K to assess the temperature induced spectral shift.

Data received from the filter vendor included room temperature spectral transmission at normal incidence and correction factors for angle of incidence and temperature. Spectral transmission data for each filter was contained in a two-column table with wavelength in the first column and transmission in the second column. Depending on the wavelength range, the

Further author information – Email: jlriens@sandia.gov; Telephone: 505-845-8682; Fax: 505-844-0906

DISCLAIMER

measurement interval was between 1 and 5 nm. A center wavelength shift factor for the specified f-number and chief ray angle and a center wavelength shift factor for 80 K were also supplied

In this paper the mathematical method used to transform the measured filter data for the system f-number and arbitrary chief ray angles is shown. The temperature shift factor supplied by the filter vendor was also included in the calculation. In principle, the transformation of measured filter data is straightforward, and the theory of interference filter properties is well covered in textbooks. The method described in this paper takes advantage of the features of a popular mathematical software package to make the calculations much less tedious. The result is a technique which can easily be applied to arbitrary f-number and chief ray angle of incidence.

The following sections of this paper cover the relevant filter theory, the analysis approach, and the application to measured filter data. Some examples of the transformation of measured filter data for various f-numbers and chief ray angles are shown.

2. INTERFERENCE FILTER PROPERTIES

Interference filters are widely used in optical systems to pass or block spectral regions of interest. These filters work on thin film interference principles to control the reflection and transmission properties at interface boundaries. Unlike absorption filters, very little of the incident energy is absorbed within the film.

The theory of interference filters is covered very well by Macleod[1]. A basic building block of filter design is a stack of many layers of the appropriate thickness and refractive index to create a highly reflecting boundary. This stack is highly reflective only for wavelengths within a certain range. This approach can be used to form either long-pass or short-pass filters. Since these filters depend on the relative phase of transmitted and reflected light, harmonics come into play. The desired long-pass or short-pass characteristics can be maintained over a limited range, and other filter layers must be used to reflect the unwanted wavelengths that are passed by the initial stack. These additional filter stacks are called blocking layers. In some cases, the filter substrate can be used as an absorption filter and block the unwanted wavelengths.

There are two basic approaches to bandpass filter design. The first approach is to combine a long-pass filter with a short-pass filter to define the spectral pass band. The other approach is to form a Fabry-Perot cavity with two reflecting stacks separated by a spacer layer. Cavity filters are used when the desired bandpass is relatively narrow compared to the center wavelength.

In the analysis of interference filters, one of the critical parameters is the phase factor for a dielectric layer. This is defined as[2]

$$\delta = \frac{2\pi n d \cos\theta}{\lambda} \tag{1}$$

where n is the index of refraction of the layer, d is the physical thickness of the layer, θ is the angle of propagation within the layer relative to normal, and λ is the wavelength of interest. A dielectric film which has a phase factor, δ, equal to $\pi/2$ is called a quarter wave film. One of the basic approaches to interference filter design is to arrange a stack of quarter wave layers with alternating high index and low index materials to form a highly reflecting assembly. The spacer layer of a cavity type bandpass filter is typically a half wave layer, with δ equal to π. The fact that δ is proportional to cos θ is key to the angle of incidence effects on interference filters.

The shift in spectral characteristics of a filter with non-collimated light is covered by Macleod[3]. His analysis is essentially the same as that of Lissberger and Wilcock[4] and of Pidgeon and Smith[5]. References 3 and 5 show that an effective index of refraction can be used to account for the change in phase upon reflection at dielectric boundaries.

To determine the angle of propagation within a film, Snell's law is used. If the angle of incidence to the filter from air or vacuum is θ_{inc} and assuming the refractive index of air is close enough to 1.00 for our purposes, then

$$\theta = \sin^{-1}\left(\frac{\sin\theta_{inc}}{n}\right) \tag{2}$$

Equation 1 is used to determine the angle of incidence effects on filter spectral characteristics. If λ_0 is the wavelength for which a certain phase factor is obtained for a dielectric layer at normal incidence, the same phase factor is obtained at non-normal incidence if the wavelength is multiplied by cos θ. Any characteristic wavelength of a filter stack, such as half-power wavelength or center wavelength, is scaled by cos θ for non-normal angle of incidence. For an assembly of layers, n_{eff} will be used with equation 2 to determine the effective angle of propagation.

$$\lambda = \lambda_0 \cos\theta$$
$$\lambda = \lambda_0 \cos\left[\sin^{-1}\left(\frac{\sin\theta_{inc}}{n_{\text{eff}}}\right)\right] \tag{3}$$

The refractive index of a film often varies with temperature, and this also affects the spectral characteristics of a filter. If the high and low index layers change proportionately with temperature, the result is a simple shift in wavelength with temperature. If the ratio of the high and low indices changes significantly with temperature, the bandwidth of a cavity type bandpass filter can also be affected.

3. ANALYSIS APPROACH

The analyses in References 3 and 5 for the effects of incident angle make use of small angle approximations and functional representations of filter transmission at normal incidence. This approach is useful for analyzing changes in center wavelength, bandwidth, and peak transmission. However, we wished to begin with measured filter transmission data and visualize how the curves would change with f-number and chief ray angle. Today's computers and user friendly mathematical software packages make a more direct, numerical integration approach feasible.

The transformation of measured filter data is accomplished in several steps. First, the geometry of a ray bundle converging toward a point on the focal plane is analyzed. This ray bundle is divided into sets of rays for which the angle of incidence on the filter is nearly equal within each set. The spectral shift induced by the angle of incidence as well as any temperature shift is then applied to the data for each set a rays. Finally, the shifted data for the all the sets are recombined using a weighting factor calculated for each set.

The geometrical analysis of the ray bundle is shown in the Appendix. The ray bundle is divided into sets of rays, and the angle of incidence within each set is θ_j, with $j = 0 \ldots (n - 1)$. The number of discrete angle increments, n, can be selected to achieve the desired degree of accuracy. The weighting factor, W_j, for each angle of incidence is also derived in the Appendix.

The spectral shift factor for each angle of incidence follows from equation 3. Angle of incidence effects always shift the spectral characteristics to shorter wavelengths. If there is a temperature shift, this can also be included.

$$S_j = \textit{temperature factor} \cdot \cos\left\{\sin^{-1}\left[\frac{\sin(\theta_j)}{n_{\text{eff}}}\right]\right\} \tag{4}$$

The next step of the filter data transformation makes use of vector and matrix operations. The measured filter data can be thought of as two vectors with the same number of elements. The first column of the data table consists of discrete wavelengths, p_i, with $i = 0 \ldots$ (m-1) and is the wavelength vector **p**. The second column of the table is the measured transmission, t_i, at each discrete wavelength and is the transmission vector **t**. The weighting factors, W_j, with $j = 0 \ldots (n - 1)$ make up the vector **W**. Similarly, the shift factors, S_j, make up the vector **S**.

For each angle of incidence (each value of j) the wavelengths of the discrete data points must be multiplied by the shift factor. This is written in matrix notation with T denoting the transpose operation.

$$\mathbf{L} = \mathbf{p} \cdot \mathbf{S}^{T} \tag{5}$$

L is a matrix with m rows and n columns. Each column represents the shifted wavelength for each data point for a given angle of incidence.

Similarly, the transmission at each data point must be multiplied by a weighting factor for each angle of incidence. This is written in matrix notation.

$$\mathbf{K} = \mathbf{t} \cdot \mathbf{W}^{T} \tag{6}$$

This is also an m x n matrix with each column representing the weighted contribution to the total transmission for each angle of incidence. Most mathematical software packages include matrix operations, so these calculations are easy to set up.

Corresponding columns of the **L** and **K** matrices represent the shifted and weighted data points for each angle of incidence. Before they are summed to obtain the transformed spectral transmission curve, the data points must be interpolated to a common set of wavelength points. The wavelengths in the original data table are convenient to use. The software package used for this work has a linear interpolation function which makes it easy to perform this operation. The format for this function is "linterp(**x**, **y**, x_i)", where the returned value is the linearly interpolated value of y_i based on the vectors **x** and **y**. If p_i is one element of the original data vector **p** and $\mathbf{L}^{\langle j \rangle}$ represents column j of matrix **L**, the transformed transmission at wavelength p_i is

$$t_{\text{trans}_i} = \sum_{j=0}^{n-1} \text{linterp}\left(\mathbf{L}^{\langle j \rangle}, \mathbf{K}^{\langle j \rangle}, p_i\right) \tag{7}$$

A simplified visual example of the result of this technique is shown in Figure 1. The total ray bundle was divided into only three sets of rays, each with a different angle of incidence. An actual transformation calculation would have many more sets of rays. The contributions from angles of incidence 1, 2, and 3 are plotted as well as the total transformed transmission. The result of this transformation technique is not the same as a simple shift in the transmission curve. The shape of the curve is affected by the range of incidence angles, and the edges of the curve become less steep.

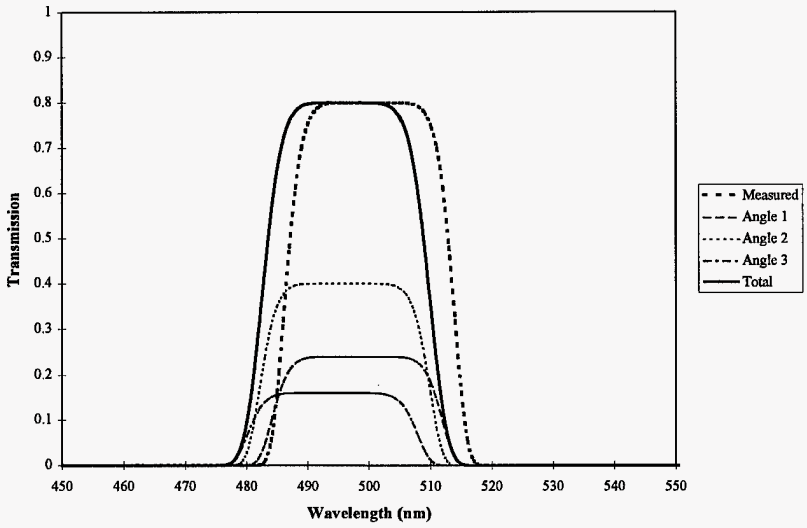

Figure 1. Example of filter data transformation

4. APPLICATION TO MEASURED FILTER DATA

The transformation technique described above was applied to measured filter data. The filter vendor made room temperature measurements with a high f-number spectroradiometer (approximately f/8) at normal incidence. The vendor had calculated from the detailed filter design the spectral shift for given f-number and chief ray angle. Using the described technique, the effective index of refraction was used as a fitting parameter to obtain the center wavelength shift for the specified chief ray angle. The vendor also measured the spectral characteristics of witness samples at room temperature and at approximately 80 K to derive a temperature shift factor.

Figure 2 shows measured filter data for a near infrared bandpass filter and the results of the transformation calculation for three different chief ray angles using an f/3 cold shield design. For this particular filter there was no appreciable temperature correction factor. The effective index of refraction was 1.775.

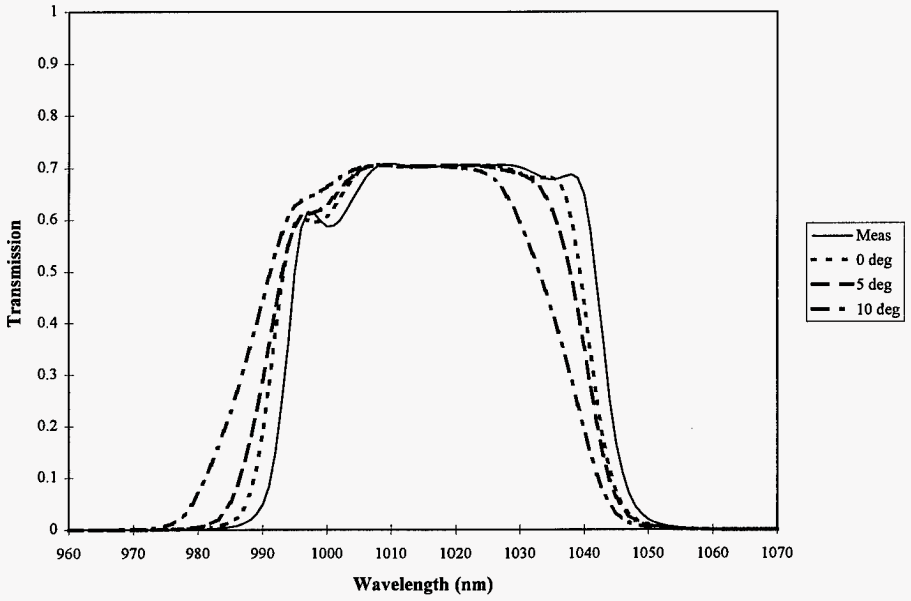

Figure 2. Transformation for three chief ray angles at f/3.

This set of curves illustrates the motivation for performing a detailed calculation of transformed filter properties. As mentioned above, the vendor had calculated the center wavelength shift for a given f-number and chief ray angle. We were interested in the shape of the transmission curve at different points on the focal plane, not just the shift. For an f/3 system the shape of the transmission curve changes substantially, particularly for chief ray angles approaching 10 degrees.

The change in filter shape and the spectral shift can be significant for small chief ray angles if the f-number is also small. Figure 3 shows transformed transmission curves for the same filter when the chief ray angle is zero and the f-number is changed. The ripple in the passband is considerably smoothed out and edges are less steep.

Figure 4 shows the transformation for a mid-wavelength infrared filter which has a significant wavelength shift with temperature. The witness sample of the filter was measured at room temperature and at approximately 80 K to determine the wavelength shift factor. The center wavelength at 80 K was found to be 0.992 times the center wavelength at room temperature. The shift from temperature effects alone is shown in the second curve. The third curve shows the combined effects of temperature and angle of incidence, using an effective index of refraction of 2.037, an f/3 optical system, and a 10 degree chief ray angle.

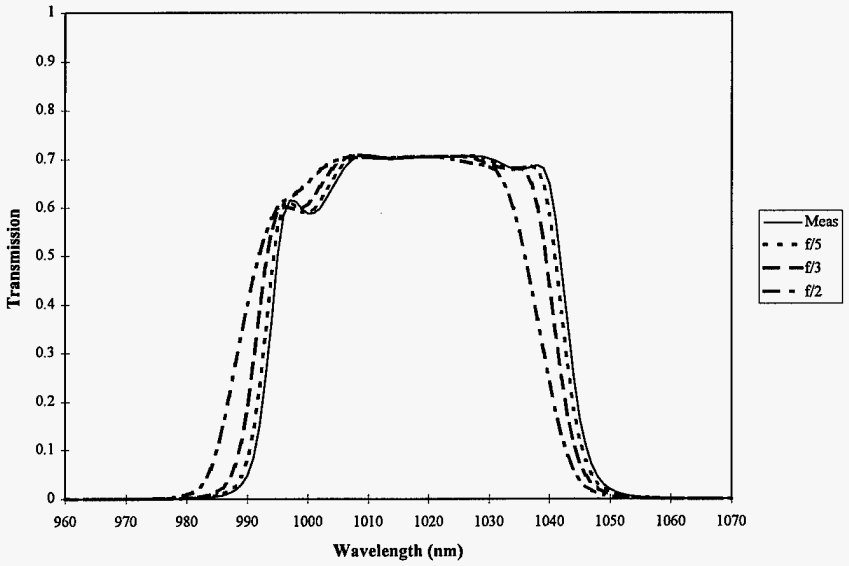

Figure 3. Transformation for three f-numbers with zero chief ray angle.

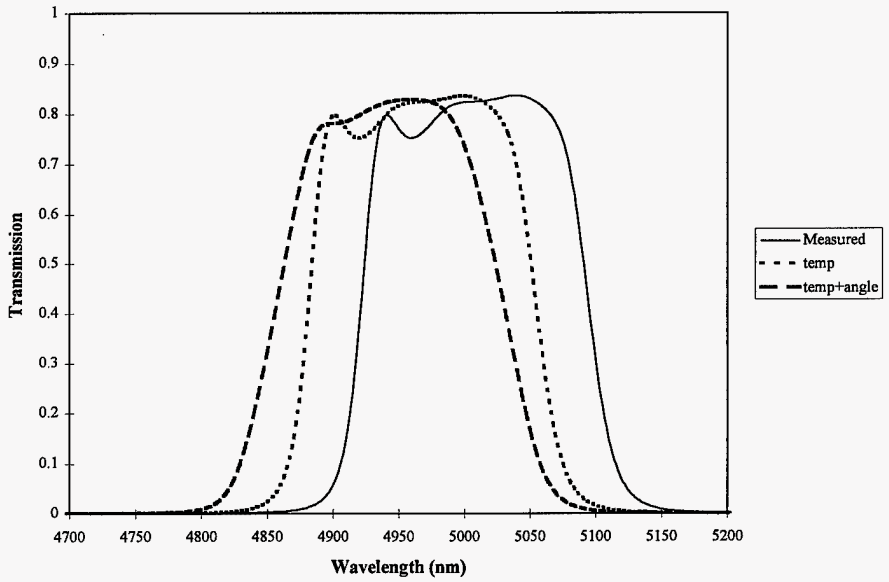

Figure 4. Transformation for f/3, 10 degree chief ray angle with temperature shift.

Once the software worksheet was set up, the detailed spectral characteristics for filters at 75 key locations on the focal plane of the multispectral sensor were calculated. Five locations within each of the 15 spectral bands were selected for analysis and comparison, and the range of chief ray angles within a given spectral band varied by as much as 8 degrees. The angle of incidence effects vary inversely with the index of refraction, and the spectral bands with the largest range of chief ray angles had the highest indices and smaller proportional changes. The worksheet proved very useful in determining if the delivered filters met our specifications and in the development of sensor data analysis algorithms. When the sensor system is completed, we plan to perform detailed spectral measurements to validate the calculated transmission curves.

5. SUMMARY

A method was described for transforming measured filter transmission data for arbitrary f-number and chief ray angle of incidence. The method is based on basic interference filter properties and takes advantage of the capabilities of a mathematical software package to make the calculations less tedious. The transformation technique begins with a determination of the shift in transmission characteristics of an interference filter with angle of incidence. A ray bundle converging to a point on the focal plane is broken down into sets of rays with nearly equal angle of incidence. A geometrical analysis of the optical system considering f-number and chief ray angle yields an expression for the weighting factor to be applied to each set of rays. The shift factors and weighting factors are applied to measured filter data for arbitrarily small incidence angle increments. Using matrix multiplication and interpolation operations built into the software package, a transformed filter transmission curve results. The transformation calculations reveal subtle changes in the shape of filter transmission curves as the f-number and chief ray angle are changed. The transformed filter curves have proven very useful in evaluating filter performance and in developing sensor data analysis tools.

6. ACKNOWLEDEMENTS

Sandia is a multiprogram laboratory operated by Sandia Corporation, a Lockheed Martin Company, for the United States Department of Energy under contract DE-AC04-94AL85000.

The author wishes to thank Sam Pellicori of Pellicori Optical Consultants and Frank Woodberry of Barr Associates for their insight and advice.

7. REFFERENCES

1. H. A. Macleod, *Thin-Film Optical Filters*, Second Edition, Chapters 2 and 6, McGraw-Hill, New York, NY, 1989.
2. Ibid., p. 33.
3. Ibid., pp. 260-269.
4. P. H. Lissberger and W. L. Wilcock, "Properties of All-Dielectric Interference Filters. II. Filters in Parallel Beams of Light Incident Obliquely and in Convergent Beams", *J. Opt Soc. Amer.* **49**, pp. 126-130, 1959.
5. C. R. Pidgeon and S. D. Smith, "Resolving Power of Multilayer Filters in Nonparallel Light", *J. Opt Soc. Amer.* **54**, pp. 1459-1466, 1964.

8. APPENDIX

The geometry of the converging ray bundle is illustrated in Figure A-1. The sensor system utilizes a cold shield to reduce the infrared background on the focal plane. The aperture of the cold shield has a diameter, d_{cs}, and is parallel to the focal plane at a distance h_{cs}. A bundle of light rays passing through the cold shield aperture converges to a point on the focal plane, and the chief ray passes through the center of the cold shield aperture. The chief ray angle, ϕ, is the angle between the chief ray and the normal to the focal plane. A filter intercepts this converging ray bundle at a height, h_f, above the focal plane. The intersection of the ray bundle with the filter plane is a circle of radius A. The expression for A is

$$A = \frac{d_{cs}}{2}\frac{h_f}{h_{cs}} \tag{A-1}$$

The radius of the ray bundle circle on the filter is independent of the chief ray angle and can be written in terms of the effective f-number of the cold shield with respect to the focal plane.

$$A = \frac{h_f}{2 \cdot f\text{-}number} \tag{A-2}$$

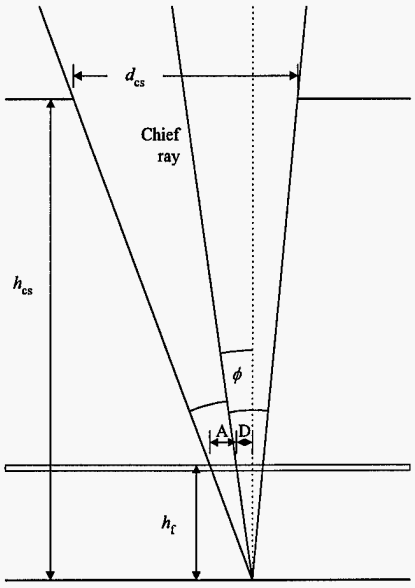

Figure A-1. Ray bundle geometry

To determine the weighting factor for each set of rays, consider Figure A-2. The arcs drawn within the circle represent the set of points for which the rays have equal angle of incidence to the filters. The angle of incidence for each value of j is θ_j. The shaded area represents an approximation for the portion of the circle for which the angle of incidence is nearly equal to θ_j.

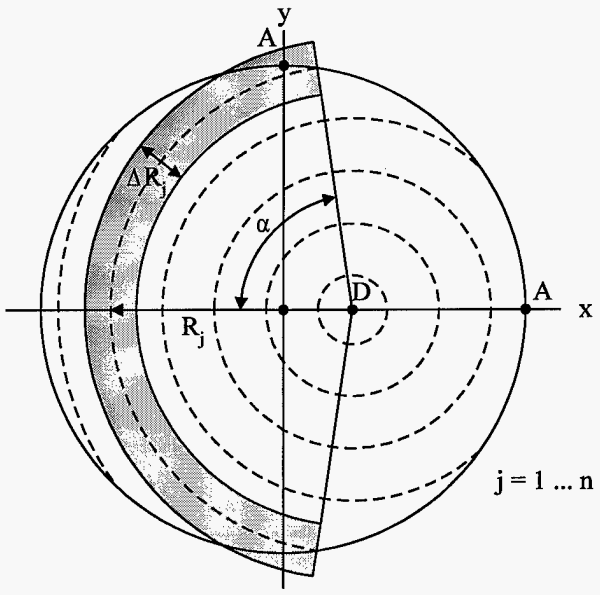

Figure A-2. Arcs of equal incidence angle

The weighting factor, W_j for angle of incidence, θ_j, is the ratio of the shaded area in Figure A-2 to the total area of the circle. The number of discrete angles to be used for the calculation can be selected. An angle increment, $\Delta\theta$, between one quarter and one half degree usually gives sufficient accuracy such that the sum of all weighting factors is very close to unity. Looking at Figures A-1 and A-2 we have the following relation for the R_j and ΔR_j.

$$R_j = h_f \tan\theta_j \tag{A-3}$$

$$\Delta R_j = h_f\left[\tan\left(\theta_j + \frac{\Delta\theta}{2}\right) - \tan\left(\theta_j - \frac{\Delta\theta}{2}\right)\right] \tag{A-4}$$

The angle, α, is determined by finding the intersection of the circle defined by the ray bundle and the arc of constant incidence angle. The center of the arc of constant incidence angle is offset from the center of the ray bundle circle by the amount

$$D = h_f \tan\phi \tag{A-5}$$

By equating the expressions for the ray bundle circle and an arc of radius R_j offset by D we can solve for x_j and y_j.

$$x_j = \frac{A^2 + D^2 - R_j^2}{2D} \tag{A-6}$$

$$y_j = \sqrt{A^2 - x_j^2} \tag{A-7}$$

The half angle of the arc is

$$\alpha_j = \tan^{-1}\left(\frac{y_j}{D - x_j}\right) \tag{A-8}$$

The equations have a real solution when x_j^2 is less than A^2. If D is less than A and R_j is less than $(A\text{-}D)$, then α_j equals π. If D is greater than A and R_j is less than $(D\text{-}A)$, then α_j is zero. Whenever R_j is greater than $(A + D)$, α_j is zero.

With all the terms defined, the weighting factor for each angle of incidence is

$$W_j = \frac{2\alpha_j R_j \Delta R_j}{\pi A^2} \tag{A-9}$$

Report Number (14) SAND--98-0667C
CONF-980412--

Publ. Date (11) 199803
Sponsor Code (18) DOE/[redacted]NN, XF
UC Category (19) UC-900, DOE/ER

DOE